ARTICLE

Pathogenic *SLIRP* variants as a novel cause of autosomal recessive mitochondrial encephalomyopathy with complex I and IV deficiency

Le Guo[1,2], Bob P. H. Engelen[3], Irene M. G. M. Hemel[3], Irenaeus F. M. de Coo[1,2], Maaike Vreeburg[4], Suzanne C. E. H. Sallevelt[4], Debby M. E. I. Hellebrekers[4], Ed H. Jacobs[5], Farah Sadeghi-Niaraki[5], Florence H. J. van Tienen[1,2], Hubert J. M. Smeets[1,2,6,7]✉ and Mike Gerards[3,7]

In a Dutch non-consanguineous patient having mitochondrial encephalomyopathy with complex I and complex IV deficiency, whole exome sequencing revealed two compound heterozygous variants in *SLIRP*. *SLIRP* gene encodes a stem-loop RNA-binding protein that regulates mitochondrial RNA expression and oxidative phosphorylation (OXPHOS). A frameshift and a deep-intronic splicing variant reduced the amount of functional wild-type *SLIRP* RNA to 5%. Consequently, in patient fibroblasts, *MT-ND1*, *MT-ND6*, and *MT-CO1* expression was reduced. Lentiviral transduction of wild-type *SLIRP* cDNA in patient fibroblasts increased *MT-ND1*, *MT-ND6*, and *MT-CO1* expression (2.5–7.2-fold), whereas mutant cDNAs did not. A fourfold decrease of citrate synthase versus total protein ratio in patient fibroblasts indicated that the resulting reduced mitochondrial mass caused the OXPHOS deficiency. Transduction with wild-type *SLIRP* cDNA led to a 2.4-fold increase of this ratio and partly restored OXPHOS activity. This confirmed causality of the *SLIRP* variants. In conclusion, we report *SLIRP* variants as a novel cause of mitochondrial encephalomyopathy with OXPHOS deficiency.

European Journal of Human Genetics (2021) 29:1789–1795; https://doi.org/10.1038/s41431-021-00947-1

INTRODUCTION

Mitochondrial encephalomyopathies (ME) are most often characterized by deficiencies in oxidative phosphorylation (OXPHOS) and ATP production, and manifest with a broad spectrum of clinical symptoms [1, 2]. Their diagnosis is challenging as a single gene defect can demonstrate a broad and complex variety of symptoms (clinical heterogeneity) and many different gene defects can result in a similar phenotype (genetic heterogeneity). The estimated number of nuclear genes involved in mitochondrial function is around 1500 of which only >250 genes have been shown to be involved in mitochondrial disease. ME is caused by variants in either the mtDNA or in a nuclear gene involved in OXPHOS [3]. However, known variants and genes only explain part of the cases. Whole exome sequencing (WES) provides the power to identify the genetic defects of ME in undiagnosed patients. Recent examples of novel ME genes, resolved by WES, are *SLC25A42* (encoding an inner mitochondrial membrane protein that imports Coenzyme A into the mitochondrial matrix) [4], *VARS2* (encoding the mitochondrial valyl tRNA-synthetase that engages in mitochondrial protein synthesis) [5], and *FBXL4* (encoding F-box and leucine-rich repeat 4 protein that controls mtDNA homeostasis and maintenance) [6]. These examples illustrate the heterogeneity in genetic causes and affected pathways in ME, which pose a challenge to an accurate molecular diagnosis of ME.

SLIRP (SRA stem-loop-interacting RNA-binding protein) plays an essential role in maintaining normal steady-state levels of all mt-mRNA transcripts encoding structural OXPHOS proteins [7]. Endogenous SLIRP predominantly resides in mitochondria and is highly expressed in energy-demanding tissues, such as brain, skeletal muscle, heart, and liver [8]. Moreover, SLIRP has also been reported to physically interact with leucine-rich pentatricopeptide repeat containing (LRPPRC) protein and to maintain normal levels of LRPPRC [9]. LRPPRC regulates mt-mRNA stability and a founder variant in the *LRPPRC* gene was shown to cause a rare French-Canadian type of Leigh syndrome (LSFC) with complex IV deficiency [10–12]. Taken together, it is suggested that SLIRP may play a role in the pathophysiology of mitochondrial diseases.

In a Dutch boy with ME, presenting as congenital hypotonia, diffuse cerebral atrophy and hypomyelination and a complex I and IV deficiency, WES revealed compound heterozygosity for two variants in the *SLIRP* gene. The pathogenicity was confirmed by a complementation assay. We showed for the first time that pathogenic variants in *SLIRP* can cause autosomal recessive ME,

[1]School for Mental Health and Neuroscience (MHeNS), Maastricht University, Maastricht, the Netherlands. [2]Department of Toxicogenomics, Clinical Genomics Unit, Maastricht University, Maastricht, the Netherlands. [3]Maastricht Center for Systems Biology (MacsBio), Maastricht University, Maastricht, the Netherlands. [4]Department of Clinical Genetics, Maastricht University Medical Center, Maastricht, the Netherlands. [5]Department of Clinical Genetics, Erasmus University Medical Center, Rotterdam, the Netherlands. [6]School for Oncology and Developmental Biology (GROW), Maastricht University, Maastricht, the Netherlands. [7]These authors contributed equally: Hubert J. M. Smeets, Mike Gerards. ✉email: bert.smeets@maastrichtuniversity.nl

Received: 8 December 2020 Revised: 9 June 2021 Accepted: 10 August 2021
Published online: 23 August 2021

adding to the genetic heterogeneity and clarifying underlying mechanisms of ME.

MATERIALS AND METHODS

Whole exome sequencing

Sequencing of the mtDNA [13] and a panel of 412 nuclear mitochondrial genes [14] did not reveal the genetic cause, therefore a WES was performed on this patient. WES was carried out and analyzed as previously described [14]. Briefly, 1 µg genomic DNA was fragmented and captured with the Agilent SureSelect Human All Exon v4 plus UTR's kit (Agilent Technologies, Amstelveen, The Netherlands) for exome enrichment. Sequencing was performed on a HiSeq 2000 Instrument (Illumina, Eindhoven, The Netherlands), and a coverage of at least 20× was achieved in more than 98% of target sequences.

Variant prioritization

Bioinformatic analysis was performed using an in-house data annotation Python/R script that matched variants to the RefGene (refGene_131114), GenCode v19 (genCode_v19_030215), and dbSNP144 hg19 tracks from the UCSC genome browser as previously described [14]. Due to an autosomal recessive inheritance, exome data of the patient were filtered for non-synonymous homozygous or compound heterozygous variants, with a minor allele frequency (MAF) below 0.01 in dbSNP144 and gnomAD, conservation by PhyloP (>1.5), and protein damage by SIFT (<0.05) and Polyphen2 (>0.85). Possible splice site variants were analyzed with SpliceSiteFinder-like, MaxEntScan, NNSPLICE and GeneSplicer. Candidate variants validation and segregation analysis was performed by Sanger sequencing using an ABI 3730 sequencer (Applied Biosystems, Bleiswijk, The Netherlands) after PCR amplification with primers listed in Supplementary Table S1. Furthermore, candidate variants were searched in available public databases including PubMed, Clinvar and the Human Gene Mutation Database (HGMD).

Functional studies

Total RNA isolation and qRT-PCR was performed as previously described [15], using primers against *SLIRP* and mtDNA-encoded subunits (primer sequences depicted in Supplementary Table S2). For TA cloning, PCR products of the patient cDNA were amplified using primers in Supplementary Table S1, and cloned into pCR2.1 vector (Thermo Fisher Scientific, Breda, the Netherlands). Positive clones were validated by Sanger sequencing. For complementation assay, *SLIRP* cDNA sequences were cloned into a lentiviral expression vector pReceiver-Lv21 (GeneCopoeia, Rockville, MD, USA) and validated by Sanger sequencing. Lentivirus was produced by co-transfecting HEK293T cells with Lenti-Pac FIV packaging plasmids (Cat. FPK-LvTR-20, GeneCopoeia) and the *SLIRP* cDNA expression vectors in a 1:1 ratio. Patient fibroblasts were infected at 70% confluence with medium containing lentiviral particles and 8 µg/ml polybrene (Sigma-Aldrich, Darmstadt, Germany). Stably transduced fibroblasts were selected with 200 µg/ml G418 (Sigma-Aldrich) for 2 weeks, starting 48 h post transduction, followed by culturing in 5 mM D-(+)-galactose (Sigma-Aldrich) supplemented DMEM (Thermo Fisher Scientific) medium for 48 h. For nonsense-mediated mRNA decay (NMD) assay, 80–90% confluent cells were treated with 100 µg/ml cycloheximide (CHX, Sigma-Aldrich) for 6 h prior to RNA isolation and qRT-PCR analysis as previously described [16]. For Western blot, anti-MT-CO1 (ab203912) (Abcam, Cambridge, UK) and anti-SDHA (ab14715) (Abcam) were used in cell lysates separated through 4–20% gradient SDS-PAGE (Bio-Rad) as previously described [17].

Database sharing of variants

SLIRP transcript NM_031210.5/ENST00000557342.6 was used for variant nomenclature and NC_000014.9 (GRCh38.p13) for exon numbering. Identified *SLIRP* variants were submitted to the Leiden Open Variation Database (individual: 00320233, DB-ID: SLIRP-000001 and SLIRP-000002) and to Clinvar (SUB9301614: SCV001519323; SUB9301630: SCV001519324).

RESULTS

Clinical history

The patient was the second child of non-consanguineous Dutch parents, born at 41 5/7 weeks after an uncomplicated pregnancy (birth weight 4.40 kg, >97th percentile) with Apgar scores being 1/5/10. Delayed progression of the delivery necessitated a cesarean section. The boy was floppy from birth and showed bouts of opisthotonic posturing. He slowly developed some motor skills, with at best reaching with his fingers to his mouth, but lost these abilities gradually around 5 months of age. After 6 months of age he developed an inspiratory stridor, a nystagmus was noted and he was difficult to console. Arms and legs were weak and not able to move against gravity (MRC 2). Reflexes could not be elicited. Tremors were seen in the muscles from head and shoulder-girdle.

Brain MRI at 9 months revealed delayed white matter maturation in the frontal and parietal regions and symmetrical in the center semi-ovale, though some maturing was seen in the occipital region. Apart from mild diffuse cerebral atrophy, no structural abnormalities were observed. Spectroscopy at 14 months did not show signs of cell loss nor a lactic acid peak in the white matter and basal ganglia voxel analyzed. Electroneurography showed a lack of sensory nerve and low compound motor action potential, which demonstrated an axonal or a mixed neuropathy. The visual evoked response via both eyes showed severe delay, fitting the visual tract defective myelination. Light and electron microscopic analysis showed no signs of hypomyelination on a sural nerve biopsy, and no abnormalities in conjunctival and rectal biopsies. The boy further deteriorated and died at 18 months from general muscle weakness with respiratory insufficiency and pneumonia.

Morphology studies on biopsy material from quadriceps muscle showed a denervation pattern. No ragged red, COX negative fibers or signs of increased histochemical staining of succinate dehydrogenase were found. Biochemical measurements of the OXPHOS complexes in quadriceps muscle biopsy and in cultured skin fibroblasts showed a deficiency of Complex I (muscle 0.06 (29%) and fibroblast 0.09 (45%) normalized to citrate synthase (CS); muscle 5.53 and fibroblast 2.41 µmol NADH/min normalized to wet protein) and Complex IV (muscle 0.57 (48%) and fibroblast 0.31 (44%) normalized to CS; muscle 50.26 and fibroblast 8.62 µmol NADH/min normalized to wet protein). The discrepancy between the histochemical staining and biochemical measurements was probably because the biopsy was obtained at a young age of the patient and histochemical abnormalities usually appear later in life [18]. Due the poor muscle quality and the death of the patient the enzyme measurement could not be repeated. Metabolic screening of blood and cerebrospinal fluid (CSF) showed a slight increase of lactate in blood (3.1 mmol/l; normal < 2.3 mmol/l) and in CSF (3.8 mmol/l; normal < 2.8 mmol/l). Amino acid, organic acid, purines and pyrimidine metabolism and sialotransferrine patterns were normal. Genetic analysis did not show chromosomal aberrations.

WES revealed two candidate variants in *SLIRP*

After filtering the WES data by allele frequency, conservation and predicted pathogenicity, three candidate genes (*TMPRSS9*, *NPC1* and *USP9Y*) remained. As variants in these genes could not explain the clinical phenotype, we included genes with one possible disease-causing variant and a clear relation to OXPHOS. The *SLIRP* gene contained a heterozygous possible disease-causing frameshift variant in exon 3 (NM_031210.5:c.248_252del; NP_112487.1:p.(Ile83Argfs*10), rs776989213, MAF = 0.000008 in dbSNP144, 0.0007% in gnomAD). Further evaluation of the *SLIRP* sequences revealed another heterozygous *SLIRP* variant (NC_000014.8:g.78177003 A > G; NM_031210.5:c.98-178 A > G, rs1402362539, MAF = 0.000016 in dbSNP144, 0.001% in gnomAD), deep in intron 1, which was reliably detected within the WES data. Both variants were extremely rare in public databases (ExAc, dbSNP144 and gnomAD), nor reported in PubMed, Clinvar and HGMD. In spite of our best effort, we could not find another case of ME patient with *SLIRP* variants. The *SLIRP* variants were

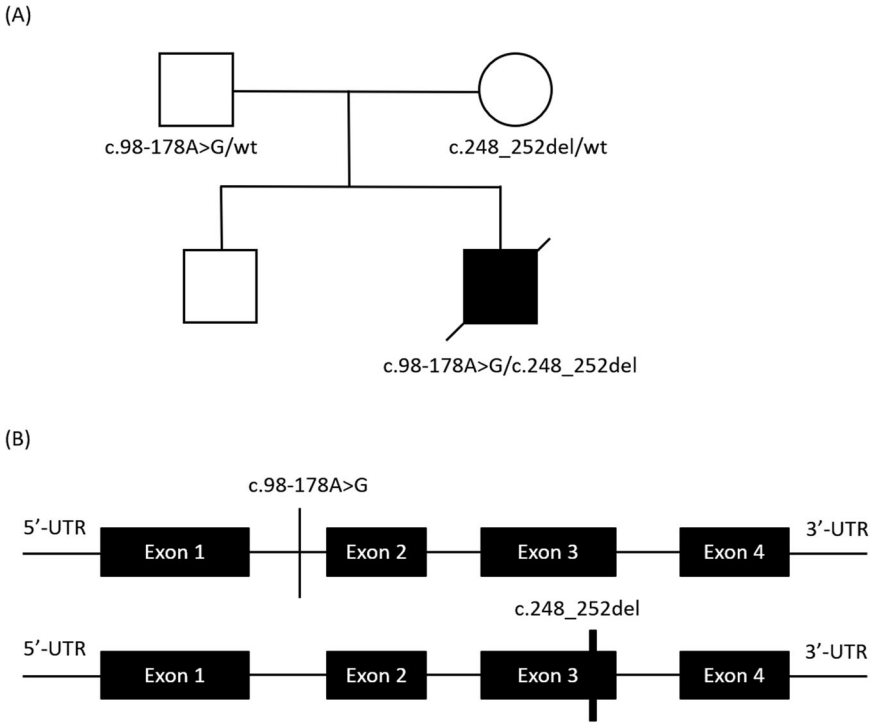

Fig. 1 Schematic view of SLIRP gene and positions of variants. A Pedigree of the index family. The index patient was diagnosed with mitochondrial encephalomyopathy as depicted by the filled black symbol. **B** Schematic diagram showing the position of two *SLIRP* mutations. Exons and introns are not drawn to scale. UTR = untranslated region.

confirmed in the patient by Sanger sequencing and both parents were carrier of one of the variants, indicating compound heterozygosity for the patient (Fig. 1). Prediction algorithms predicted the c.98-178 A > G variant creates a novel cryptic 5′′ splice site 106 nt downstream of a high-scoring potential cryptic 3′ splice site (Fig. 2A).

Effect of *SLIRP* variants at the fibroblast RNA level

Two *SLIRP* cDNA products were detected in the patient cDNA, one of the expected size and one larger (Fig. 2B). TA cloning and Sanger sequencing revealed three different cDNA fragments. The largest fragment showed retention of a 106 bp fragment of intron 1 (r.97_98ins98-283_98-178, Fig. 2C), leading to a frameshift and premature stop codon (NP_112487.1:p.(Ser33Argfs*9)) due to the *SLIRP* c.98-178 A > G variant. The normal-sized fragment consisted of *SLIRP* cDNA with the deletion-type and the wild-type. qRT-PCR was performed using primer pairs to capture overall *SLIRP* expression and each transcript type (wild-type, deletion-type, and insertion-type) separately (Supplementary Fig. 1A). Forward primer (Fq1) in exon 2 and reverse primer (Rq1) in exon 3 showed a decrease of overall *SLIRP* expression to 63% of controls (Supplementary Fig. 1B). Forward primer (Fq2) in exon 3 and reverse primer (Rq2) encompassing the 5 bp deletion in exon 3 quantified wild-type and insertion-type *SLIRP* mRNA as 16% of controls (Supplementary Fig. 1B). Forward primer (Fq3) spanning the exon 1-exon 2 boundary and primer (Rq3) in front of the exon 3 deletion determined the level of wild-type and deletion-type transcripts as 52% of controls (Supplementary Fig. 1B). From these data we calculated that in the patient, 74% is deletion-type, 18% is insertion-type and only a small minority (8%) is wild-type (Supplementary Fig. 1C). As the *SLIRP* expression is overall decreased to 63%, only 5% of wild-type *SLIRP* RNA is present in the patient fibroblasts. CHX treatment did not increase overall, wild-type and deletion-type, wild-type and insertion-type *SLIRP* mRNA expression in patient fibroblasts (Supplementary Fig. 1D).

Wild-type *SLIRP* transduction rescues mtDNA gene expression and OXPHOS enzyme activity

SLIRP facilitates the association of mt-mRNAs with the mitoribosome [9]. In fibroblasts of the patient, qRT-PCR showed a decrease of mt-mRNA transcripts *MT-CO1*, *MT-ND1, MT-ND6*, and *MT-CYB* (Fig. 3A, Supplementary Fig. 2). SLIRP has been reported to physically interact with leucine-rich pentatricopeptide repeat containing (LRPPRC) protein and to maintain normal levels of LRPPRC [9]. The level of LRPPRC mRNA transcripts was decreased to 76% in the patient fibroblasts, although not statistically significant (Fig. 3A). A complementation assay was performed in patient fibroblasts, which were stably transduced with lentiviral clones containing cDNA from wild-type *SLIRP*, *SLIRP* containing the deletion, and *SLIRP* containing the 106 bp intron 1 retention. Complex IV *MT-CO1* RNA expression in patient fibroblasts transduced with wild-type *SLIRP* showed a 7.2-fold increase (***, $p < 0.001$) and complex I *MT-ND1* and *MT-ND6* a 2.5- and 4.2-fold increase (Fig. 3B), respectively, compared to non-transduced patient fibroblasts. The increased expression of *MT-CYB* was not significant (Fig. 3B). Neither the deletion-type *SLIRP* nor insertion-type *SLIRP* increased expression of these genes (Fig. 3B).

The enzyme activity of CS and OXPHOS complex I and IV was measured in the patient fibroblasts before and after complementation with wild-type *SLIRP*. The CS versus protein ratio in the patient cells was 27% of the controls, which suggested a mitochondrial depletion (Fig. 3C). After transfection with wild-type *SLIRP* cDNA, the CS versus protein ratio increased to 64% of control values. Related to the protein level, complex I activity in patient fibroblasts was fully restored by wild-type *SLIRP*, and complex IV partly (Fig. 3C).

Moreover, protein levels of MT-CO1 and SDHA were measured in the patient fibroblasts before and after complementation with wild-type *SLIRP* cDNA. The MT-CO1/SDHA protein ratio showed a 40–50% decrease in patient fibroblasts, which was improved by transduction with the wild-type *SLIRP* cDNA (Fig. 3D).

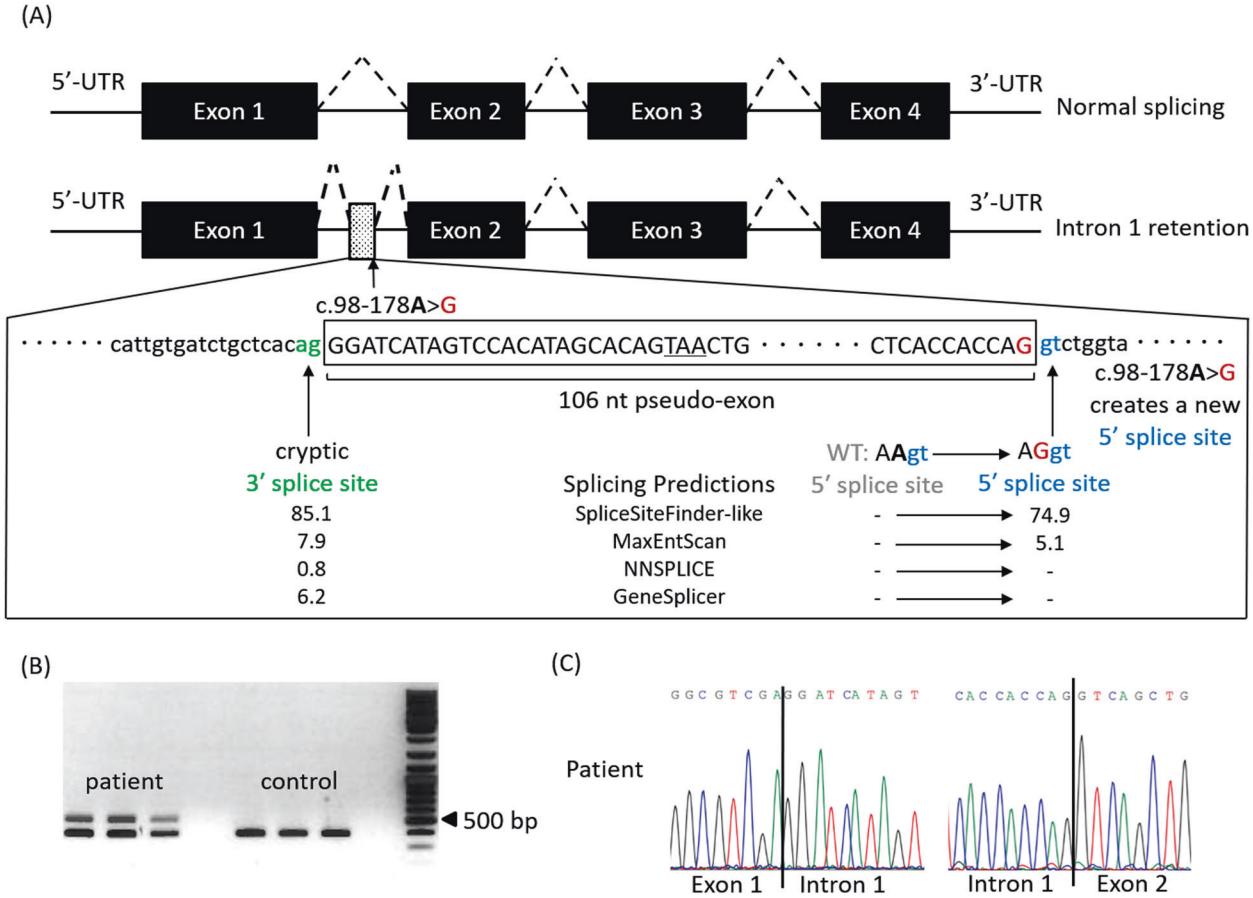

Fig. 2 The effects of *SLIRP* mutations on RNA level. A Schematic diagram of the abnormal splicing event induced by the *SLIRP* c.98-178 A > G variant, showing the positions of the novel 5′ and 3′ cryptic splice site and the encoded stop codon resulting from partial retention of intron 1. Exons and introns are not drawn to scale. **B** PCR product of entire *SLIRP* cDNA. The control showed the expected wild-type size, whereas the patient had an additionally larger transcript product ($n = 3$). **C** Sequence analysis after cloning patient *SLIRP* cDNA revealed a 106 bp retention from intron 1 due to the c.98-178 A > G variant in *SLIRP* gene.

DISCUSSION

The *SLIRP* c.248_252del and c.98-178 A > G variants were identified by WES in a non-consanguineous Dutch patient as a novel cause of ME. Initially, the *SLIRP* gene was missed due to the presence of only one possible pathogenic variant in the predefined region of interest (exons and their 100 bp flanking intronic regions). As none of the genes with two potentially pathogenic variants could explain the clinical symptoms, WES data was reanalyzed for OXPHOS-related genes with one possible disease-causing variant (rare in our routine WES analysis). *SLIRP* was such a candidate. Endogenous SLIRP predominantly resides in mitochondria and is highly expressed in energy-demanding tissues, such as brain, skeletal muscle, heart and liver, suggesting the role of SLIRP in the pathophysiology of mitochondrial diseases [8]. SLIRP was first described as an RNA-binding protein that interacts with the STR7 substructure of steroid-receptor RNA-activator [8]. SLIRP harbors two ubiquitination sites (Lys36, Lys88) within an RNA recognition motif domain (Ala21-Val91), which is essential for correct association of mt-mRNAs with the mitoribosome [9, 19–21]. Subsequently, a second deep-intronic variant in *SLIRP* intron 1 was detected with a predicted effect on splicing. Total *SLIRP* mRNA expression was reduced to 63% in patient fibroblasts compared to controls. Analysis of *SLIRP* transcripts showed that the majority of *SLIRP* transcripts was deletion-type (74%), followed by insertion-type (18%) and wild-type (8%). The reduced level of total *SLIRP* transcripts and the low level of insertion-type *SLIRP* transcripts suggested NMD for the c.98-178 A > G variant, but not for the c.248_252del variant with the premature stop codon in the last exon. CHX treatment did not increase overall, wild-type and deletion-type, wild-type and insertion-type *SLIRP* mRNA expression in patient fibroblasts, therefore NMD of *SLIRP* mRNA expression could not be demonstrated. As different mechanisms of NMD exist, we still consider it likely that NMD is the cause of the imbalance in transcripts, but further experiments are needed to demonstrate or exclude NMD unequivocally. Corrected for the overall decrease in expression to 63%, indicated that only 5% wild-type *SLIRP* transcripts were present compared to controls. The other two transcripts would not yield a functional protein.

SLIRP is an OXPHOS regulator, maintaining steady-state levels of mtDNA-encoded transcripts [7]. In *SLIRP* knockout mice, SLIRP was involved in presenting mature mRNAs to the mitoribosome to fine-tune mitochondrial protein synthesis [9]. In SLIRP knockout mice a drastic decrease in mt-mRNA transcripts was observed, in line with the decrease of *MT-ND1*, *MT-ND6, MT-CYB* and *MT-CO1* RNA in fibroblasts of our patient. *MT-ND6* RNA was only slightly decreased to 79%, which may be due to the relatively small size and short half-life compared to the other mt-mRNA transcripts [22, 23]. SLIRP physically interacts with LRPPRC and protects the latter from degradation by mitochondrial matrix proteases [9]. The locations of LRPPRC-SLIRP binding sites are conserved through evolution [24]. LRPPRC regulates mt-mRNA stability and a recessive missense variant Ala354Val in the *LRPPRC* gene was shown to cause LSFC [10–12]. Although LSFC and ME are both early-onset mitochondrial disorders with severe clinical presentations, different clinical evolution appears in LSFC patients that characterized by progressive neurodegeneration and acute

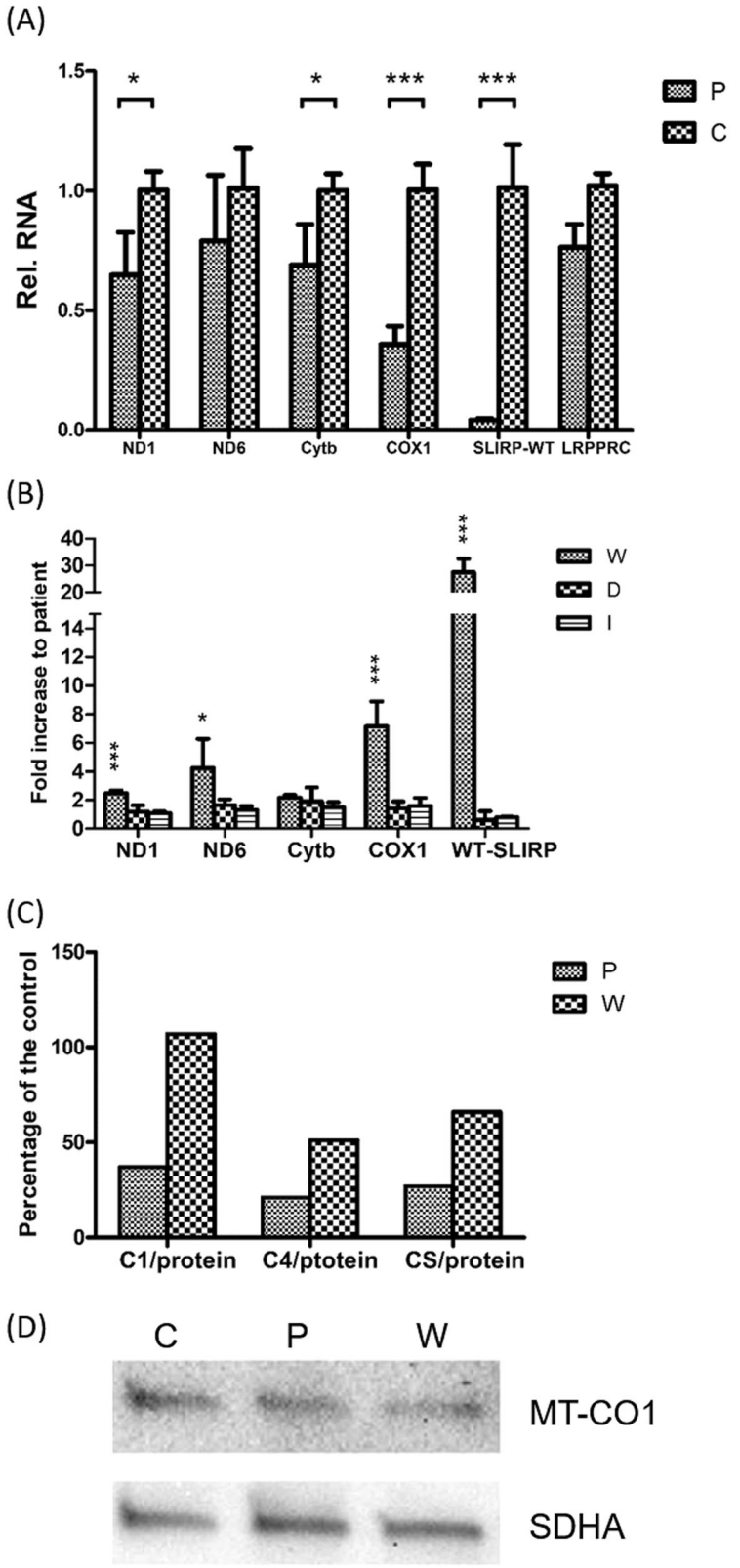

acidosis, while our ME patient showed a delayed neurodevelopment and a slight increase of lactate in blood and CSF. In addition, LSFC patients exhibited isolated complex IV deficiency in skin fibroblasts and combined complex I and IV deficiencies in skeletal muscle, while our ME patient showed a biochemical defect of complex I and IV in both fibroblasts and skeletal muscle. SLIRP and LRPPRC form a ribonucleoprotein complex that promotes the posttranscriptional expression of mt-mRNA transcripts and both proteins are co-stabilized within the complex [7, 22]. In our patient, the levels of *LRPPRC* mRNA transcripts decreased to 76%

Fig. 3 Complementation assay of SLIRP in patient fibroblasts. A Mitochondrial transcript steady-state levels assessed by qPT-PCR in patient fibroblasts (denoted as P) and controls (denoted as C). *hTBP* was used as endogenous control. Data are represented as means ± SD ($n = 3$). Error bars indicate SD. Student's *t* test was used for statistics. *$p < 0.05$, **$p < 0.01$, ***$p < 0.001$. **B** Transduction of patient fibroblasts with wild-type *SLIRP* recovers mitochondrial gene expression in galactose medium culture. Patient fibroblasts were stably transduced with lentiviral clones containing wild-type *SLIRP* (denoted as W), *SLIRP* containing 5 bp deletion in exon 3 (denoted as D) and *SLIRP* containing 106 bp intron 1 retention (denoted as I). *hTBP* was used as endogenous control. Relative RNA expressions of W, D and I were normalized to P. The relative RNA expression data are represented as means ± SD ($n = 3$). Error bars indicate SD. Student's *t* test was used for statistics. *$p < 0.05$, **$p < 0.01$, ***$p < 0.001$. **C** Transduction of patient fibroblasts with wild-type *SLIRP* restored complex I and IV activity. The enzyme measurement was performed once because of the extremely early senescence of the transfected cells, which prohibited culturing to sufficiently large numbers of cells. **D** Transduction of patient fibroblasts with wild-type *SLIRP* partially restored *MT-CO1* protein levels.

compared to control fibroblasts (though not statistically significant). As the predominant deletion variant c.248_252del is located downstream to key amino acids (His59, Arg60, Glu80, Asn81 and His82) for LRPPRC-SLIRP interaction, this may cause limited damage to the LRPPRC-SLIRP binding interface [25].

In our patient, a decrease in mtDNA-encoded transcripts, a decreased CS/protein ratio and a combined complex I and IV deficiency were detected in muscle and fibroblasts. Transduction with wild-type *SLIRP* cDNA caused an increase in mtDNA-encoded transcripts, such as *MT-CO1*, *MT-ND1* and *MT-ND6*, whereas this did not happen when transduced with the deletion-type *SLIRP* cDNA or insertion-type *SLIRP* cDNA. Transduction with the wild-type *SLIRP* cDNA also caused an increase in mitochondrial mass per cell (increased CS/protein ratio) and an increase in complex I and IV activity, when normalized for the amount of protein. Moreover, MT-CO1/SDHA protein ratio was decreased in patient fibroblasts, which was improved by transduction with the wild-type *SLIRP* cDNA.

The two *SLIRP* variants were classified as likely pathogenic according to ACMG criteria [26], leading to autosomal recessive ME:

Strong evidence of pathogenicity (PS3): Wild-type SLIRP transduction rescued mtDNA gene expression (increased mt-mRNA transcripts and MT-CO1/SDHA protein ratio) and OXPHOS enzyme activity (increased complex I and IV enzyme activity), which was demonstrated in the complementation assay.

Moderate evidence of pathogenicity (PM2): Both variants are not present in PubMed, ClinVar or HGMD and only extremely low frequency as heterozygote in dbSNP144 and gnomAD. The splicing variant (NC_000014.8:g.78177003 A > G; NM_031210.5:c.98-178 A > G, rs1402362539) has an MAF of 0.000016 in dbSNP144 and 0.001% in gnomAD. The deletion variant (NM_031210.5: c.248_252del; NP_112487.1:p.(Ile83Argfs*10), rs776989213) has an MAF of 0.000008 in dbSNP144 and 0.0007% in gnomAD.

Supporting evidence of pathogenicity (PP1): Both variants in the patient were segregated within this family.

Supporting evidence of pathogenicity (PP3): Both variants affect highly conserved amino acids. The deletion variant is predicted to be pathogenic according to SIFT and Polyphen2. The splicing variant is predicted to create a novel cryptic 5′ splice site.

WES is a powerful tool to identify the majority of variants that cause mitochondrial diseases [14]. Still, due to technical issues and location of variants outside the captured regions, pathogenic variants will be missed. A recent study reported an additional 10% (5 of 48) increase of diagnostic rate by RNA sequencing in molecularly undiagnosed mitochondrial patients [27]. Although most mitochondrial genes are ubiquitously expressed, nuclear encoded mitochondrial genes can have imbalanced expression in rare situation, like *SLIRP* gene in our case. Imbalanced expression of *SLIRP* alleles was discovered by analyzing RNA in our patient fibroblasts, indicating that RNA sequencing would have discovered *SLIRP* as a candidate gene. RNA sequencing is therefore an important complementary tool to identify rare, disease-causing variants in mitochondrial diseases, but it should be realized that RNA sequencing is limited to genes that are expressed in the cells or tissue studied.

REFERENCES

1. Russell OM, Gorman GS, Lightowlers RN, Turnbull DM. Mitochondrial diseases: hope for the future. Cell. 2020;181:168–88.
2. Rahman S. Mitochondrial disease in children. J Intern Med. 2020;287:609–33.
3. Thompson K, Collier JJ, Glasgow RIC, Robertson FM, Pyle A, Blakely EL, et al. Recent advances in understanding the molecular genetic basis of mitochondrial disease. J Inherit Metab Dis. 2020;43:36–50.
4. Almannai M, Alasmari A, Alqasmi A, Faqeih E, Al Mutairi F, Alotaibi M, et al. Expanding the phenotype of SLC25A42-associated mitochondrial encephalomyopathy. Clin Genet. 2018;93:1097–102.
5. Bruni F, Di Meo I, Bellacchio E, Webb BD, McFarland R, Chrzanowska-Lightowlers ZMA, et al. Clinical, biochemical, and genetic features associated with VARS2-related mitochondrial disease. Hum Mutat. 2018;39:563–78.
6. Gai X, Ghezzi D, Johnson MA, Biagosch CA, Shamseldin HE, Haack TB, et al. Mutations in FBXL4, encoding a mitochondrial protein, cause early-onset mitochondrial encephalomyopathy. Am J Hum Genet. 2013;93:482–95.
7. Baughman JM, Nilsson R, Gohil VM, Arlow DH, Gauhar Z, Mootha VK. A computational screen for regulators of oxidative phosphorylation implicates SLIRP in mitochondrial RNA homeostasis. PLoS Genet. 2009;5:e1000590.
8. Hatchell EC, Colley SM, Beveridge DJ, Epis MR, Stuart LM, Giles KM, et al. SLIRP, a small SRA binding protein, is a nuclear receptor corepressor. Mol Cell. 2006;22:657–68.
9. Lagouge M, Mourier A, Lee HJ, Spahr H, Wai T, Kukat C, et al. SLIRP Regulates the Rate of Mitochondrial Protein Synthesis and Protects LRPPRC from Degradation. PLoS Genet. 2015;11:e1005423.
10. Ruzzenente B, Metodiev MD, Wredenberg A, Bratic A, Park CB, Cámara Y, et al. LRPPRC is necessary for polyadenylation and coordination of translation of mitochondrial mRNAs. EMBO J. 2012;31:443–56.
11. Sasarman F, Brunel-Guitton C, Antonicka H, Wai T, Shoubridge EA, Consortium L. LRPPRC and SLIRP interact in a ribonucleoprotein complex that regulates post-transcriptional gene expression in mitochondria. Mol Biol Cell. 2010;21:1315–23.
12. Mootha VK, Lepage P, Miller K, Bunkenborg J, Reich M, Hjerrild M, et al. Identification of a gene causing human cytochrome c oxidase deficiency by integrative genomics. Proc Natl Acad Sci. 2003;100:605–10.
13. Spruijt L, Smeets HJ, Hendrickx A, Bettink-Remeijer MW, Maat-Kievit A, Schoonderwoerd KC, et al. A MELAS-Associated ND1 Mutation Causing Leber Hereditary Optic Neuropathy and Spastic Dystonia. Arch Neurol. 2007;64:890–3.
14. Theunissen TEJ, Nguyen M, Kamps R, Hendrickx AT, Sallevelt S, Gottschalk RWH, et al. Whole Exome Sequencing Is the Preferred Strategy to Identify the Genetic Defect in Patients With a Probable or Possible Mitochondrial Cause. Front Genet. 2018;9:400.
15. Nguyen M, Boesten I. Hellebrekers DMEI, Vanoevelen J, Kamps R, de Koning B, et al. Pathogenic CWF19L1 variants as a novel cause of autosomal recessive cerebellar ataxia and atrophy. Eur J Hum Genet. 2016;24:619–22.
16. Durand C, Roeth R, Dweep H, Vlatkovic I, Decker E, Schneider KU, et al. Alternative splicing and nonsense-mediated RNA decay contribute to the regulation of SHOX expression. PLoS ONE. 2011;6:e18115.
17. van den Bosch BJ, Gerards M, Sluiter W, Stegmann AP, Jongen EL, Hellebrekers DM, et al. Defective NDUFA9 as a novel cause of neonatally fatal complex I disease. J Med Genet. 2012;49:10–5.
18. Lehtonen JM, Auranen M, Darin N, Sofou K, Bindoff L, Hikmat O, et al. Diagnostic value of serum biomarkers FGF21 and GDF15 compared to muscle sample in mitochondrial disease. J Inherit Metab Dis. 2021;44:469–80.
19. Wagner SA, Beli P, Weinert BT, Nielsen ML, Cox J, Mann M, et al. A proteome-wide, quantitative survey of in vivo ubiquitylation sites reveals widespread regulatory roles. Mol Cell Proteomics. 2011;10:M111.013284.
20. Beltrao P, Albanèse V, Kenner LR, Swaney DL, Burlingame A, Villén J, et al. Systematic functional prioritization of protein posttranslational modifications. Cell. 2012;150:413–25.
21. Stes E, Laga M, Walton A, Samyn N, Timmerman E, De Smet I, et al. A COFRADIC protocol to study protein ubiquitination. J Proteome Res. 2014;13:3107–13.

22. Chujo T, Ohira T, Sakaguchi Y, Goshima N, Nomura N, Nagao A, et al. LRPPRC/SLIRP suppresses PNPase-mediated mRNA decay and promotes polyadenylation in human mitochondria. Nucleic Acids Res. 2012;40:8033–47.
23. Bruni F, Proctor-Kent Y, Lightowlers RN, Chrzanowska-Lightowlers ZM. Messenger RNA delivery to mitoribosomes—hints from a bacterial toxin. FEBS J. 2021;288:437–51.
24. Siira SJ, Spahr H, Shearwood AJ, Ruzzenente B, Larsson NG, Rackham O, et al. LRPPRC-mediated folding of the mitochondrial transcriptome. Nat Commun. 2017;8:1532.
25. Spahr H, Rozanska A, Li X, Atanassov I, Lightowlers RN, Chrzanowska-Lightowlers ZM, et al. SLIRP stabilizes LRPPRC via an RRM-PPR protein interface. Nucleic Acids Res. 2016;44:6868–82.
26. Richards S, Aziz N, Bale S, Bick D, Das S, Gastier-Foster J, et al. Standards and guidelines for the interpretation of sequence variants: a joint consensus recommendation of the American College of Medical Genetics and Genomics and the Association for Molecular Pathology. Genet Med: Off J Am Coll Med Genet. 2015;17:405–24.
27. Kremer LS, Bader DM, Mertes C, Kopajtich R, Pichler G, Iuso A, et al. Genetic diagnosis of Mendelian disorders via RNA sequencing. Nat Commun. 2017;8:15824.

ACKNOWLEDGEMENTS

The authors are grateful to all participants for their involvement.

AUTHOR CONTRIBUTIONS

LG, BPHE, MG contributed to the design of the research. LG wrote the manuscript. LG, BPHE, MG analysed the WES data. LG, BPHE, IMGMH performed the cellular experiments. MV, SCEHS, DMEIH provided the clinical data. EHJ, FSN performed the OXPHOS measurements. FHJT, HJMS, MG were involved in planning and supervised the work. All authors discussed the results and commented on the manuscript.

FUNDING

This study was supported by funding from China Scholarship Council (Grant Number: 201606310036) and Neuromusculair en Mitochondrieel Onderzoek (NeMO) foundation (Grant/Award Number: 19_P02). Part of this work has been supported by the Dutch Province of Limburg.

COMPETING INTERESTS

The authors declare no competing interests.

ETHICAL APPROVAL

Follow-up investigations to confirm the genetic diagnosis were performed in accordance with the regulations of the local ethical committee of Maastricht University Medical Centre.

INFORMED CONSENT

Subjects gave written informed consent for WES analysis in accordance with the Declaration of Helsinki as part of their clinical/molecular genetics diagnosis at Maastricht University Medical Centre.

ADDITIONAL INFORMATION

Supplementary information The online version contains supplementary material available at https://doi.org/10.1038/s41431-021-00947-1.

Correspondence and requests for materials should be addressed to H.J.M.S.

Reprints and permission information is available at http://www.nature.com/reprints

Publisher's note Springer Nature remains neutral with regard to jurisdictional claims in published maps and institutional affiliations.